ECONOMIC GEOLOGY

RESEARCH UNIT

University of the Witwatersrand

Johannesburg

— • —

ON THE RELATIONSHIP BETWEEN CUMULUS MINERALOGY
AND TRACE AND ALKALI ELEMENT CHEMISTRY
IN AN ARCHAEAN GRANITE FROM THE
BARBERTON REGION, SOUTH AFRICA

T.S. McCARTHY and L.J. ROBB

ON THE RELATIONSHIP BETWEEN CUMULUS MINERALOGY AND TRACE AND ALKALI ELEMENT CHEMISTRY IN AN ARCHAEAN GRANITE FROM THE BARBERTON REGION, SOUTH AFRICA

by

T. S. McCARTHY

(Lecturer, Department of Geology, University of the Witwatersrand)

and

L. J. ROBB

(Assistant Research Officer, Economic Geology Research Unit)

ON THE RELATIONSHIP BETWEEN CUMULUS MINERALOGY

AND TRACE AND ALKALI ELEMENT CHEMISTRY

IN AN ARCHAEAN GRANITE FROM THE

BARBERTON REGION, SOUTH AFRICA

ABSTRACT

The Ba, Sr, Rb, K_2O and Na_2O contents of cumulates formed during the *in situ* fractional crystallization of a granitic magma are examined. Fractionation involving the assemblage plagioclase-quartz-biotite followed by plagioclase-quartz-biotite-K-feldspar are considered in theoretical models and in a natural example from the Barberton Mountain Land, South Africa. During plagioclase-quartz-biotite fractionation, Ba and Rb enrich in successive solids and melt, while Sr is depleted. The K_2O content of the solid phase is very different from that of the melt while Na_2O contents are similar so that variations in the amount of intercumulus melt result in wide variation in the Na_2O/K_2O ratio. The K/Rb ratio decreases, and K/Ba increases. The incoming of K-feldspar as a cumulus phase causes Ba to be depleted along with Sr in successively formed solids, while Rb continues to be enriched. A pronounced compositional hiatus with respect to trace elements results. The K_2O and Na_2O contents of melt and cumulate are now similar, so that little scatter in Na_2O/K_2O ratio occurs as a result of variation in the amount of intercumulus melt. A rapid fall in K/Rb occurs, while K/Ba shows a marked increase. In general, trace element data from the natural example fit the models well, although the observed scatter of the data is somewhat greater than predicted by simple variation in cumulus-intercumulus proportions. A possible cause related to non-uniform distribution of biotite is considered.

* * * * * * * * * * * * * * * * * * *

ON THE RELATIONSHIP BETWEEN CUMULUS MINERALOGY
AND TRACE AND ALKALI ELEMENT CHEMISTRY
IN AN ARCHAEAN GRANITE FROM THE
BARBERTON REGION, SOUTH AFRICA

CONTENTS

———————] [———————

ON THE RELATIONSHIP BETWEEN CUMULUS MINERALOGY

AND TRACE AND ALKALI ELEMENT CHEMISTRY

IN AN ARCHAEAN GRANITE FROM THE

BARBERTON REGION, SOUTH AFRICA

I. INTRODUCTION

Fundamental to the development of our present understanding of plutonic, basic and ultrabasic complexes has been our knowledge of both fractional crystallization and processes of segregation of melt and solid during crystallization. These concepts have not been widely applied to deep-seated magmatic granitic rocks. This is not surprising, as such rocks usually lie near the minimum melt composition in the granite system, and thus resemble liquids (Winkler, 1976). In addition, igneous sedimentary structures, which are indicative of fractional crystallization, are uncommon in granitic rocks, although some have been described (Emeleus, 1963; Smith, 1974). Furthermore, distinct cumulus-intercumulus textural relationships are not normally observed in granites.

The majority of authors reporting research results on granites have assumed *in situ* crystallization by essentially an equilibrium mode, although most admit to some fractional crystallization having occurred, usually prior to emplacement. McCarthy and Hasty (1976) have, in contrast, suggested on a basis of trace element data, that many granites have a cumulate character - the result of *in situ* fractional crystallization.

Experimental work has shown (Winkler, 1976) that increasing water pressure causes the cotectic line in the granite system to move towards more feldspathic compositions. Therefore, a granitic melt produced at high pressure will, on rising in the crust, undergo plagioclase + quartz (+ mafic mineral) followed by plagioclase + quartz + K-feldspar (+ mafic mineral) crystallization. In the event of fractional crystallization taking place, such a change in cumulus mineralogy would be expected to have a marked influence on trace element distribution patterns in the resultant solids. This paper explores the consequences of such a change on the Ba, Rb and Sr distribution, as well as on K_2O and Na_2O abundances in theoretical models, and relates these to a natural example.

II. THEORETICAL MODELS

Gravity segregation of crystals from granitic melts is evidently rare. Fractionation rather occurs by a progressive, inward, nucleation of crystals from the margins of the magma chamber (Wolhuter, 1973). This process is well-illustrated by the freezing of a very dilute (5 ppm) aqueous gentian violet solution. Slow diffusion of ions in the solid state prevents re-equilibration between early formed solids and melt, while the melt, in contrast, remains more-or-less homogeneous in composition. In this paper, we refer to crystals which form by this process as "cumulus" crystals, and to trapped interstitial melt as "intercumulus" melt, since chemically they are likely to be indistinguishable from their respective gravity-segregated counterparts. We assume that intercumulus melt crystallizes in isolation from the main mass of magma.

Various equations have been derived which describe the behaviour of trace elements during fractional crystallization (Neumann et al., 1954; Greenland, 1970; McCarthy and Hasty, 1976). Of these, the Rayleigh law (Neumann et al., 1954) is the most simple, and will be used here.

A knowledge of crystal/melt partition coefficients is prerequisite to modelling trace element behaviour. Most partition coefficients for minerals found in granites are derived from phenocryst/matrix pairs, and much uncertainty surrounds this data limiting the precision of the models. In this work, the partition coefficients compiled by McCarthy (1976) have been used, except in the case of the partition coefficient of Ba in biotite, where a value of 6,0 has been adopted following Condie and Hunter (1976).

A granitic melt lying on the quartz-plagioclase cotectic surface will undergo fractionation of these two minerals in approximately equal proportions. A mafic mineral will normally crystallize as well. The effect on Rb, Sr and Ba contents of a melt as a result of such crystallization (in this case including minor biotite) is shown in Figure 1 by curves AB. Because Ba and Rb are partitioned into the melt, their abundance increases with fractionation, while that of Sr decreases, as this element is strongly partitioned into plagioclase. The trace element composition of the solid phase separating from the melt will change continuously, and will lie along the curve DE (Figure 1).

Fractionation of plagioclase and quartz (plus mafic mineral) will continue until the K-feldspar phase volume is reached, whereupon the separation of a potassic feldspar in addition to plagioclase and quartz (and a mafic mineral), will commence. This has a marked influence on the
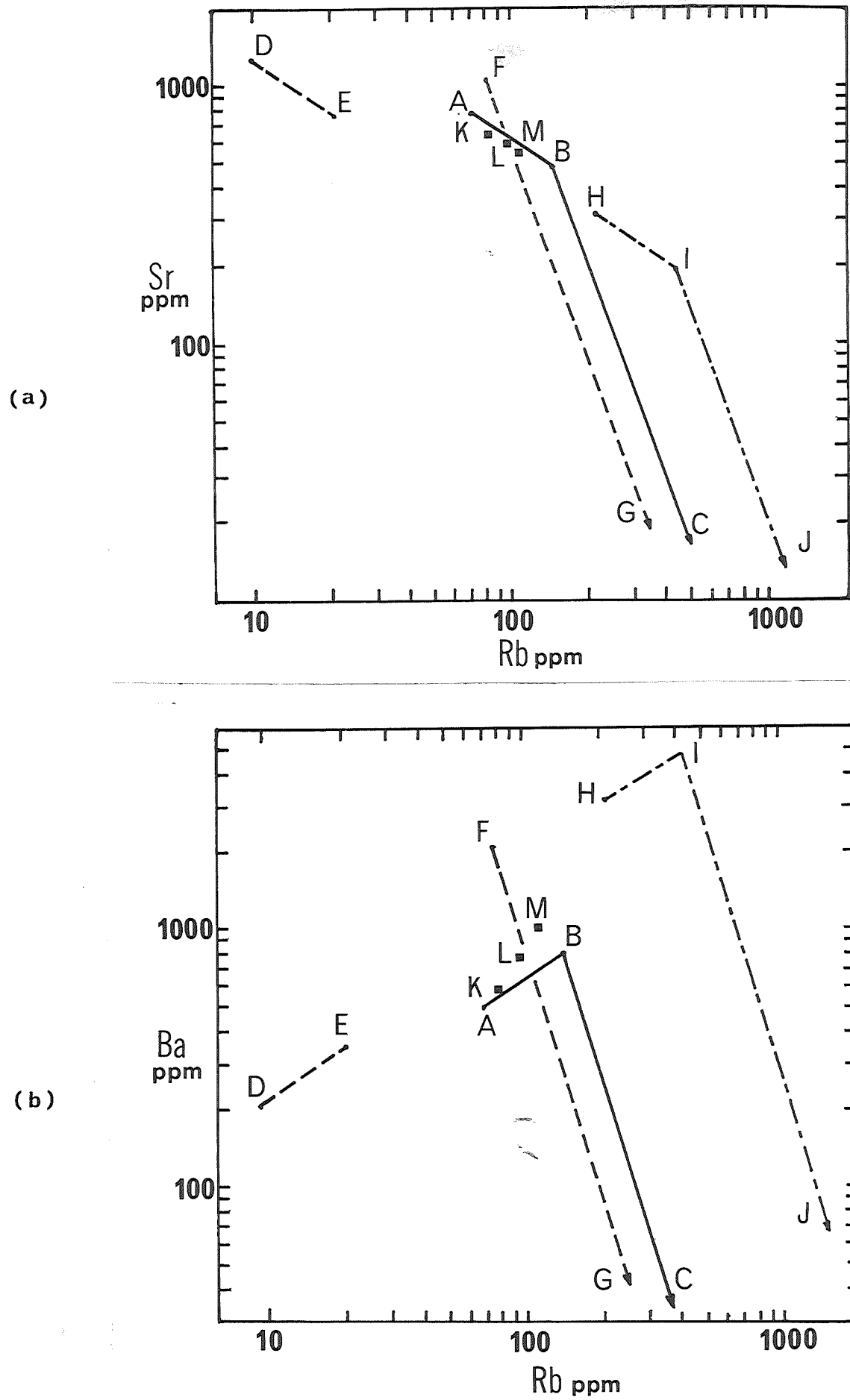
Figure 1 : *The effect of fractional crystallization on Sr and Rb (a) and Ba and Rb (b) contents of a granitic melt. Initial melt is at A. From this melt, 47% plagioclase, 49% quartz and 4% biotite are fractionally removed, causing the liquid to move towards B. The composition of the solid phase lies along DE. At B, which represents 55% crystallization of melt A, the liquidus mineralogy changes to 32% plagioclase, 28% quartz, 30% K-feldspar and 10% biotite. The liquid composition now changes towards C, and the fractionally separated solid compositions lie along FG. HI represents the compositions of biotite in equilibrium with melts along AB, and IJ biotites in equilibrium with melts along BC. K is the composition of a 50-50 mix of E and B; L a 5% addition of biotite I to K, and M a 10% addition of biotite I to K.*

trace element distribution, because both Sr and Ba are strongly partitioned into K-feldspar. This effect is illustrated in Figure 1, where at point B, which represents 55 per cent crystallization of melt A, K-feldspar appears on the liquidus. From this point, crystallization of quartz, plagioclase, and K-feldspar occurs in approximately equal proportions (together with biotite). The melt now changes composition along BC (Figure 1). The first solid, containing cumulus K-feldspar, to separate from liquid B has composition F, and subsequent solids lie along FG. Ba is now actively removed from the melt, while Sr is more strongly removed than previously, because of the greater quantity of feldspar in the cumulus assemblage. Thus, the two sets of fractionation trends have distinctly different slopes.

The model predicts that a distinct compositional hiatus will exist in the solid at the point where K-feldspar becomes a liquidus phase. However, as pointed out by McCarthy and Hasty (1976) perfect separation of cumulus crystals from a melt is unlikely, and some trapped intercumulus melt may be anticipated. This will result in solids lying between pure melt and pure cumulate trends on Figure 1, and will result in a partial closing of the compositional hiatus. Actual solid composition in the two branches will lie scattered within the two parallelograms ABED and FBCG respectively. In the former case, this may give the appearance of a trend from D to B, rather than one parallel to AB.

The presence of intercumulus liquid will have a marked effect on the alkali contents of rocks forming in the plagioclase-quartz (plus mafic mineral) fractionation branch. The Na_2O content of this cumulus assemblage is similar to that of the melt, so that variation in the amount of trapped intercumulus melt will have only a small effect on the Na_2O content. By contrast, the K_2O content of the cumulus assemblage is considerably lower than that of the liquid, and varies only slightly as crystallization proceeds, while that of the melt increases with fractionation. The inter-relationships between trace elements and K_2O content for plagioclase-quartz (plus biotite) fractionation in a mixed cumulus-intercumulus assemblage (i.e. a whole rock) are portrayed in Figure 2. Assuming that the initial magma contained some 3.0% K_2O, and that the cumulus assemblage contained 1.0% K_2O, lines of constant K_2O content in mixed cumulus - intercumulus assemblages have been calculated and are shown superimposed on the Rb, Ba and Sr relationships for plagioclase-quartz fractionation in Figure 2. The slight increase in K_2O content of the solid with fractionation has been neglected. Because of increasing K_2O content in the liquid with increasing fractionation, the more fractionated the system, the less intercumulus melt required to produce a given K_2O content in a mixed assemblage. Hence, the constant K_2O content lines are asymptotic on the cumulate composition line. Therefore, along a line of constant cumulus-intercumulus proportions (e.g. AB, Figure 2), the K_2O content will increase. Because the quantity of inter-cumulus melt is likely to be high, an increase in K_2O will be observed down a trend on a Ba or Sr vs Rb plot.

The K_2O content of a mixed cumulus-intercumulus assemblage resulting from plagioclase-quartz (plus mafic mineral) fractionation will be strongly influenced by the amount of intercumulus melt and the degree of fractionation of the system. Therefore, it follows that marked variation in Na_2O/K_2O ratios are to be expected, ranging from high values (around 5) in the cumulus-rich material to low values (around 1) in melt-rich samples.

It is appropriate at this point to consider the consequences that the models here discussed have for the K/Rb and K/Ba ratios. In Figure 3, point A represents a melt (having a K/Rb ratio of 350 and a K_2O content of 3%) which undergoes plagioclase-quartz (with minor biotite) fractionation. The cumulus assemblage is assumed to contain a constant 1% K_2O. The first solid to separate lies at point D. With progressive crystallization, the melt changes composition towards B, while the cumulate moves towards E (ignoring the normal slight increase in K_2O). Lines showing the composition of mixed assemblages, containing 10, 20, and 40% trapped melt are shown on Figure 3. It is evident from this figure that variations in the amount of intercumulus melt will result in wide scatter in the data, although a general decrease in K/Rb with increasing K_2O should be discernible.

At point B (Figure 3), which represents approximately 55% crystallization, K-feldspar becomes a cumulus phase, the latter accompanied by an assumed slight increase in the biotite content. The assumed cumulus assemblage contains 6% K_2O, while the melt contains 5.5% K_2O. The first K-feldspar-bearing solid to separate from melt B lies at F. A distinct change in K/Rb now occurs and fractionation leads to a significant drop in K/Rb, in both the melt, which moves towards C, and the solid, which changes in the direction of G. The composition of a mixed cumulus-intercumulus assemblage containing 20% intercumulus melt (NP) is shown in Figure 3.

From the data presented in Figure 3, it may be inferred that the branch involving only intercumulus K-feldspar will, in general, exhibit more scatter and will have higher K/Rb ratios than that involving cumulus K-feldspar.

The model-derived K/Ba vs K_2O relationships are portrayed in Figure 4. As discussed in relation to Figure 3, plagioclase-quartz (plus biotite) fractionation from melt A causes the melt composition to increase in K/Ba towards B whilst the equilibrium cumulates lie along DE. The entry of K-feldspar causes a depletion of Ba and a concomittant increase in K/Ba towards C. The K-feldspar-bearing cumulates lie along FG.
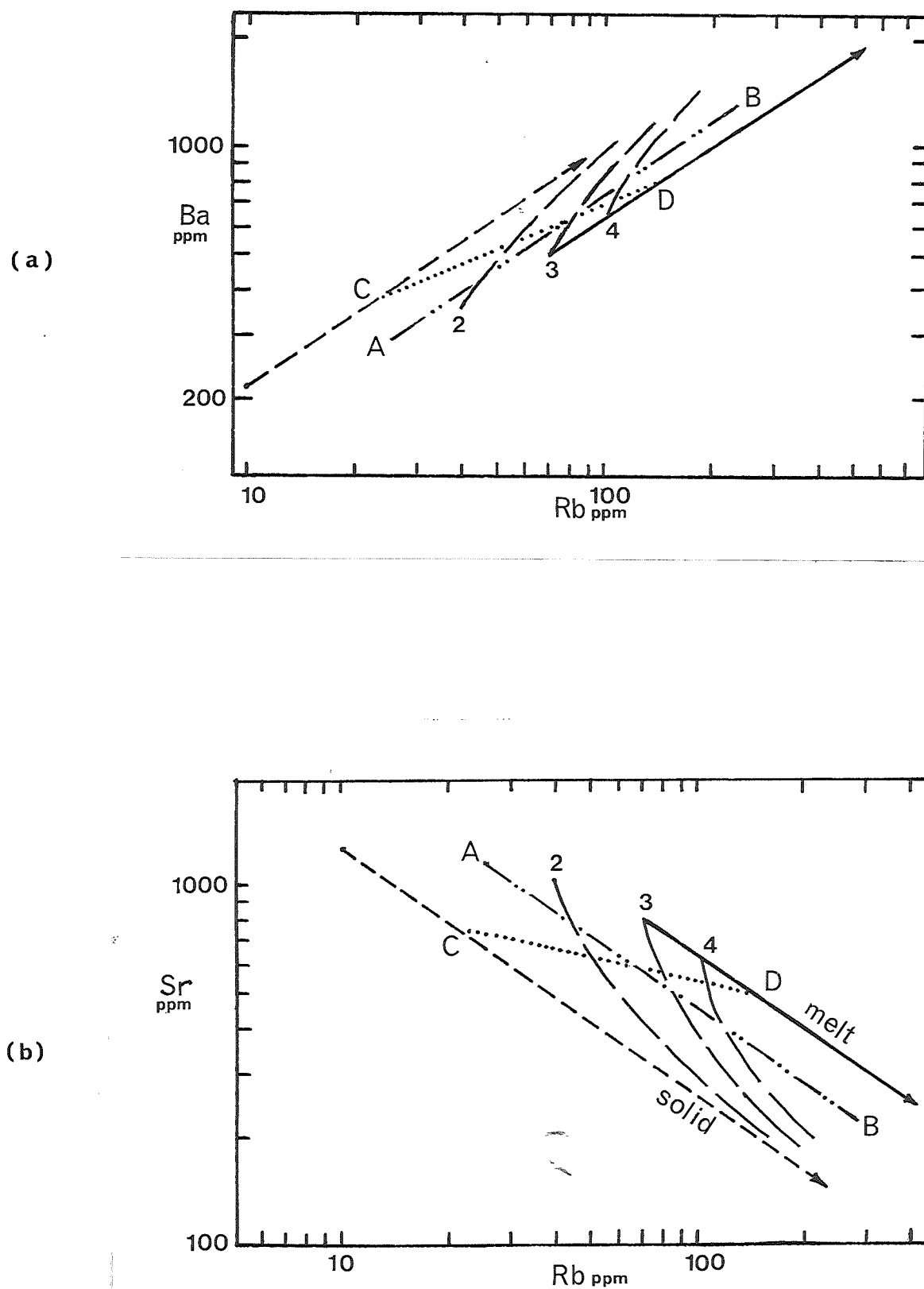
<u>Figure 2</u> : *The relationship between Ba and Rb (a), Sr and Rb (b), and K₂O contents in a mixed cumulus - intercumulus assemblage during plagioclase-quartz-biotite fractionation. The Ba, Rb and Sr curves are reproduced from Figure 1. It is assumed that the initial melt contained 3% K₂O, and that the separating solid contained a constant 1% K₂O. Lines of constant K₂O content (2, 3, and 4%) in mixed cumulus-intercumulus assemblages are shown. Compositions containing 25% intercumulus melt lie along AB. The line CD is the locus of compositions of mixed assemblages which may form at 55% solidification of the original magma.*

In summary, a change in cumulus mineralogy from plagioclase-quartz (plus mafic mineral) to plagioclase-K-feldspar-quartz (plus mafic mineral) results in the following chemical features :

(a) Ba and Rb initially increase in abundance in the solid and melt, while Sr decreases, until K-feldspar crystallization is initiated, whereupon Ba and Sr decrease in abundance (Figure 1).
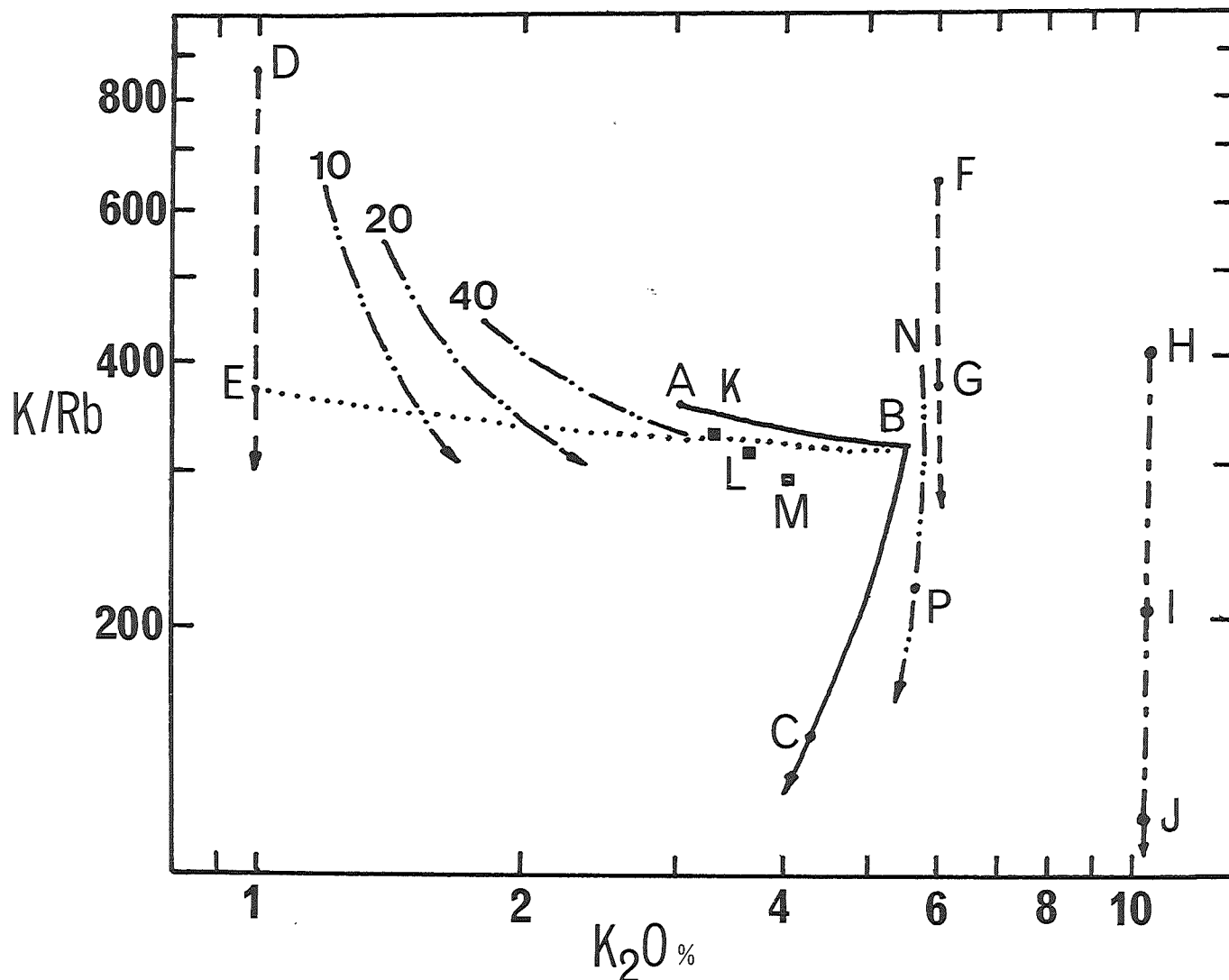
Figure 3 : *The relationship between K/Rb ratio and K_2O content during the fractional crystallization discussed in relation to Figures 1 and 2. Initial magma composition is at A. This fractionates plagioclase (47%), quartz (49%), and biotite (4%). The first solid to form is assumed to contain 1% K_2O and lies at D. Subsequent solids lie along DE. The melt evolves along AB. The loci of composition of mixed cumulus-intercumulus assemblages containing 10%, 20% and 40% intercumulus melt are shown. Curve EB is the locus of mixed assemblages which may form at 55% crystallization of melt A. At B, cumulus mineralogy changes to plagioclase (32%), K-feldspar (30%), quartz (28%) and biotite (10%). The first solid lies at F, and subsequent solids lie along FG. The melt evolves towards C. NP is the locus of compositions containing 20% intercumulus melt. Biotites in equilibrium with melts along AB lie along HI (assuming a constant 10,5% K_2O in biotite), while biotites in equilibrium with melts BC lie along IJ. K is a 50-50 mix of melt B and cumulate E, and L is a mixture of 5% biotite I with K; M is a mixture of 10% biotite I with K.*

(b) The melt compositions are continuous, but exhibit inflections at the point where K-feldspar becomes a cumulus mineral, while the solids (cumulate) shows distinct compositional hiatuses (Figure 1).

(c) The presence of variable amounts of intercumulus melt will result in a tendency towards merging of the two trends.

(d) The Na_2O/K_2O ratio is likely to vary widely when K-feldspar is present only as an intercumulate phase, while a more restricted range in Na_2O/K_2O ratio will occur once K-feldspar is a cumulus mineral.
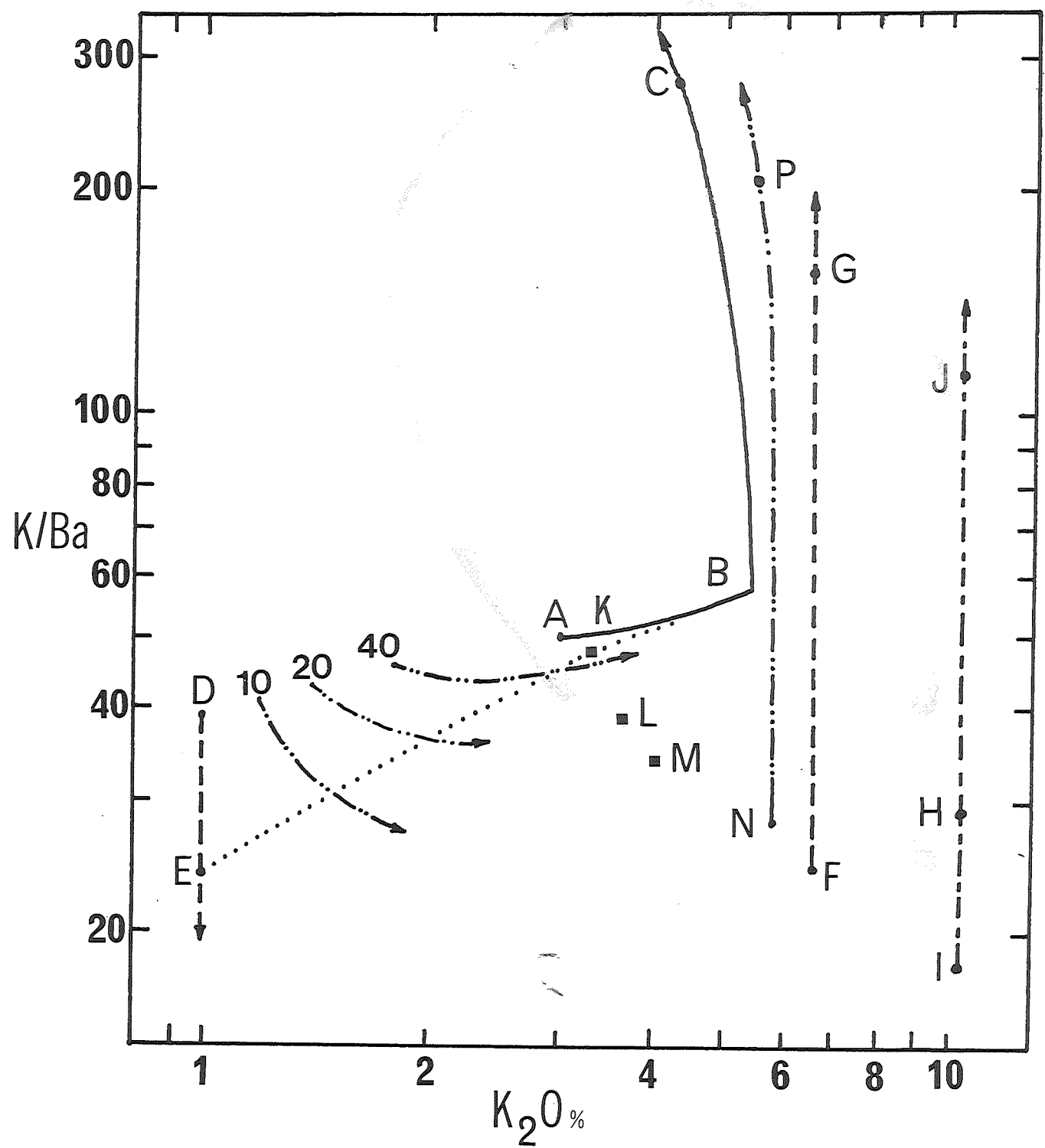
Figure 4 : *The relationship between K/Ba and K₂O. The points on this plot are analogous to those on Figure 3.*

III. A CASE STUDY FROM THE ARCHAEAN OF SOUTH AFRICA

(a) General Geological Description

The Archaean granitic terrane north of the Barberton Mountain Land (Figure 5) has previously been termed the Nelspruit Granite (Visser and Verwoerd, 1960; Hunter, 1974) and the Nelspruit Migmatite terrane (Viljoen and Viljoen, 1969). These authors described this terrane as consisting of a sequence of migmatites and gneisses, often porphyritic in character and considerably more potassic than the tonalitic diapirs that intrude the Barberton greenstone belt.
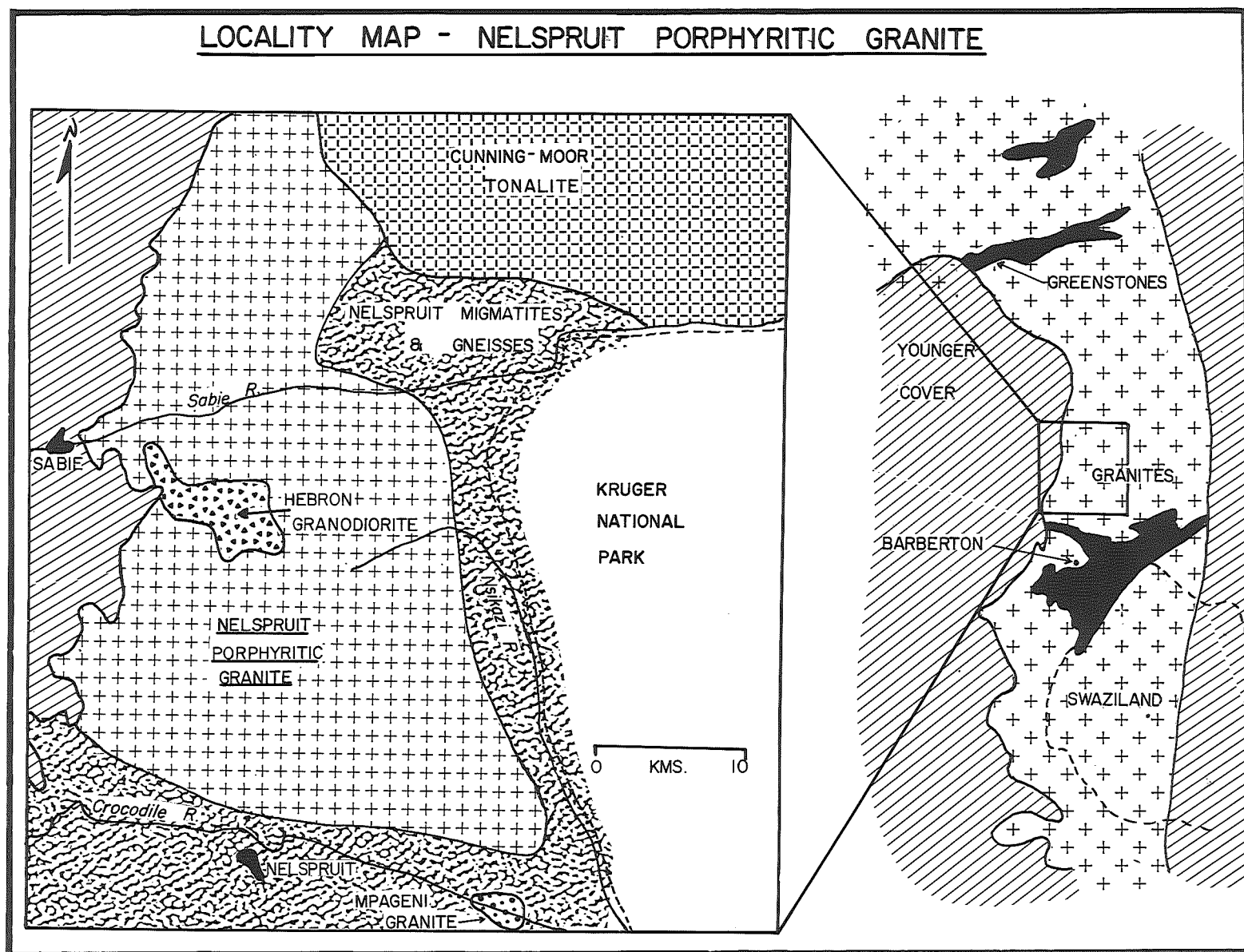

Figure 5 : *Locality map showing the distribution of the Nelspruit porphyritic granite .*

Recent mapping in the area to the north of the Mountain Land has revealed considerable complexity and a number of granitic types have been recognized (Robb, 1977). Most of the region is underlain not by migmatites, but by a porphyritic granite termed the *Nelspruit Porphyritic Granite* (Figure 5). This porphyritic granite has been intruded by the Hebron granodiorite, the Cunning-Moor tonalite and the Mpageni granite pluton. Migmatites and gneisses are exposed in the major river valleys whereas the Nelspruit Porphyritic Granite is generally confined to higher lying areas. This suggests that the latter has a sheet-like character and in this respect resembles the "Hood" or Lochiel Granite described to the south of the Mountain Land (Viljoen and Viljoen, 1969; Hunter, 1973).

The Nelspruit porphyritic granite consists essentially of large (up to 3 cms in length) poikilitic microcline microperthitic phenocrysts set in a groundmass of medium- to coarse-grained quartz, alkalic plagioclase, and minor biotite. Although the degree of phenocryst development is variable the granite is recognizable as a single unit over some 2 500 kms^2.

Recent geochronological work (Erika Barton, personal communication, 1977) has yielded an Rb-Sr whole rock age of 3 205 ± 49 m.y. (R_0 = 0,7016 ± 0,0004) for the Nelspruit Porphyritic Granite.

(b) Analytical Techniques

Seventy-nine samples of porphyritic granite were partially analyzed by X-ray fluorescence spectrometry, the oxides K_2O and Na_2O and trace elements Rb, Sr, and Ba being determined. Ba, Rb, Sr, and Na_2O were determined in the manner described by McCarthy (1976) although mass absorption corrections were omitted since calibration was carried out against granitic standards. K_2O was determined on whole rock pellets following the method of Cherry et al. (1970). Precision and accuracy are the same as those listed by McCarthy (1976).

(c) Results

Two distinct compositional types occur within the Nelspruit Porphyritic Granite. The first of these is characterized by an inverse correlation between Sr and Rb (Figure 6), a positive
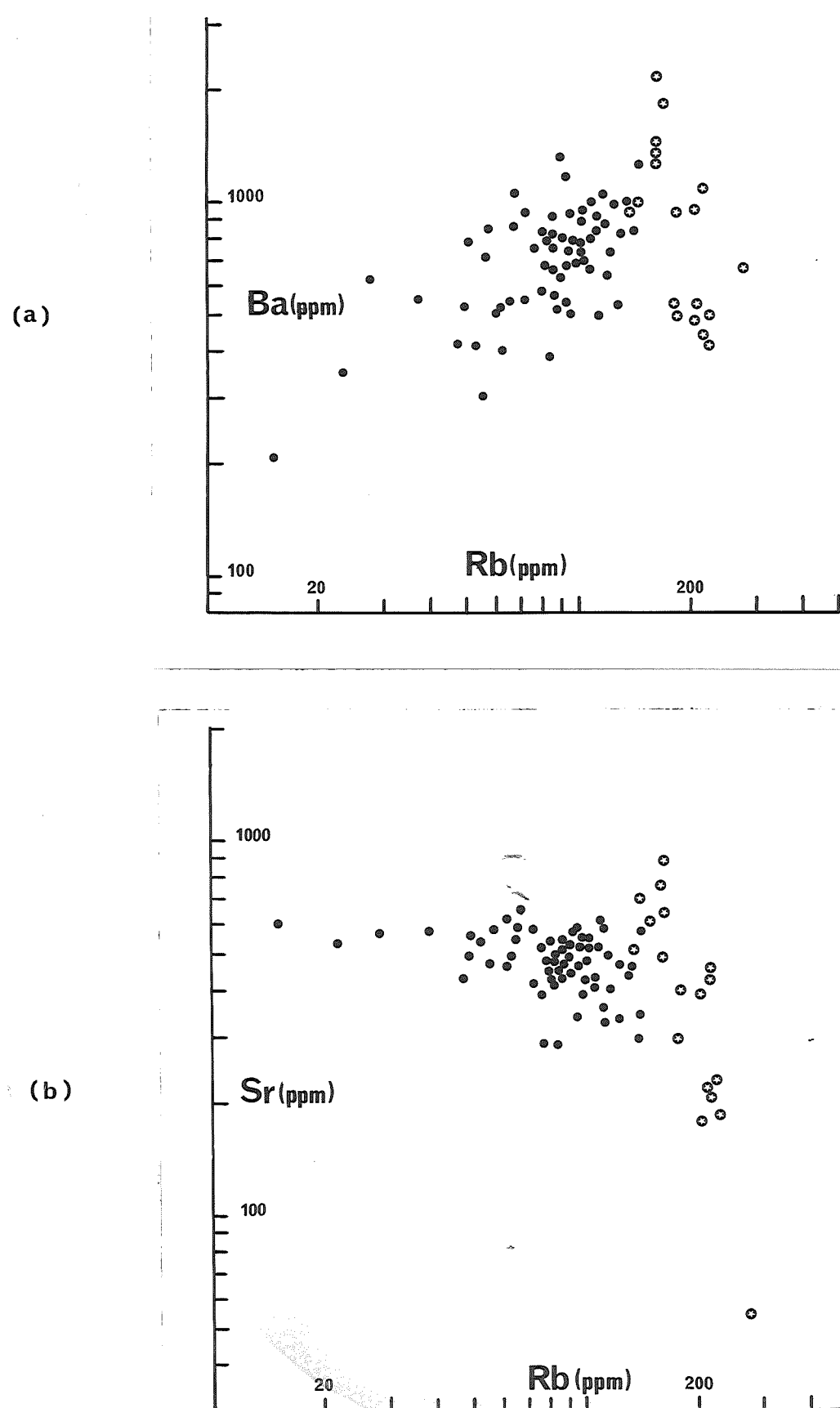

Figure 6 : *The Ba and Rb (a) and Sr and Rb (b) relationships in the Nelspruit Porphyritic Granite. The different symbols denote the two varieties of granite. The solid symbols represent the plagioclase-quartz-biotite fractionation branch, whereas the open symbols represent the plagioclase-quartz-biotite-K-feldspar fractionation branch.*

correlation between Ba and Rb (Figure 6) and a wide range in Na_2O/K_2O proportions (Figure 7). The second group exhibits inverse Sr vs Rb and Ba vs Rb trends (Figure 6), is more potassic than the first (Figure 7), and has a more restricted range in Na_2O/K_2O proportions (Figure 7). On a plot of K/Rb ratio against K_2O content (Figure 8), the two types are resolved, the first having a higher K/Rb ratio and exhibiting more scatter, both with respect to K/Rb and K_2O, than the second. On a plot of K/Ba vs K_2O (Figure 9) the first type has a more restricted range in K/Ba than the second. Finally, within the first type, there is a tendency towards increasing K_2O with increasing Rb and decreasing Sr (Figure 10). The two types of Nelspruit Porphyritic Granite are not clearly distinguishable in hand-specimen, although the second variety tends to be more biotite-rich (approximately 10% modal vs 4% modal) and also has a more clearly defined porphyritic texture.
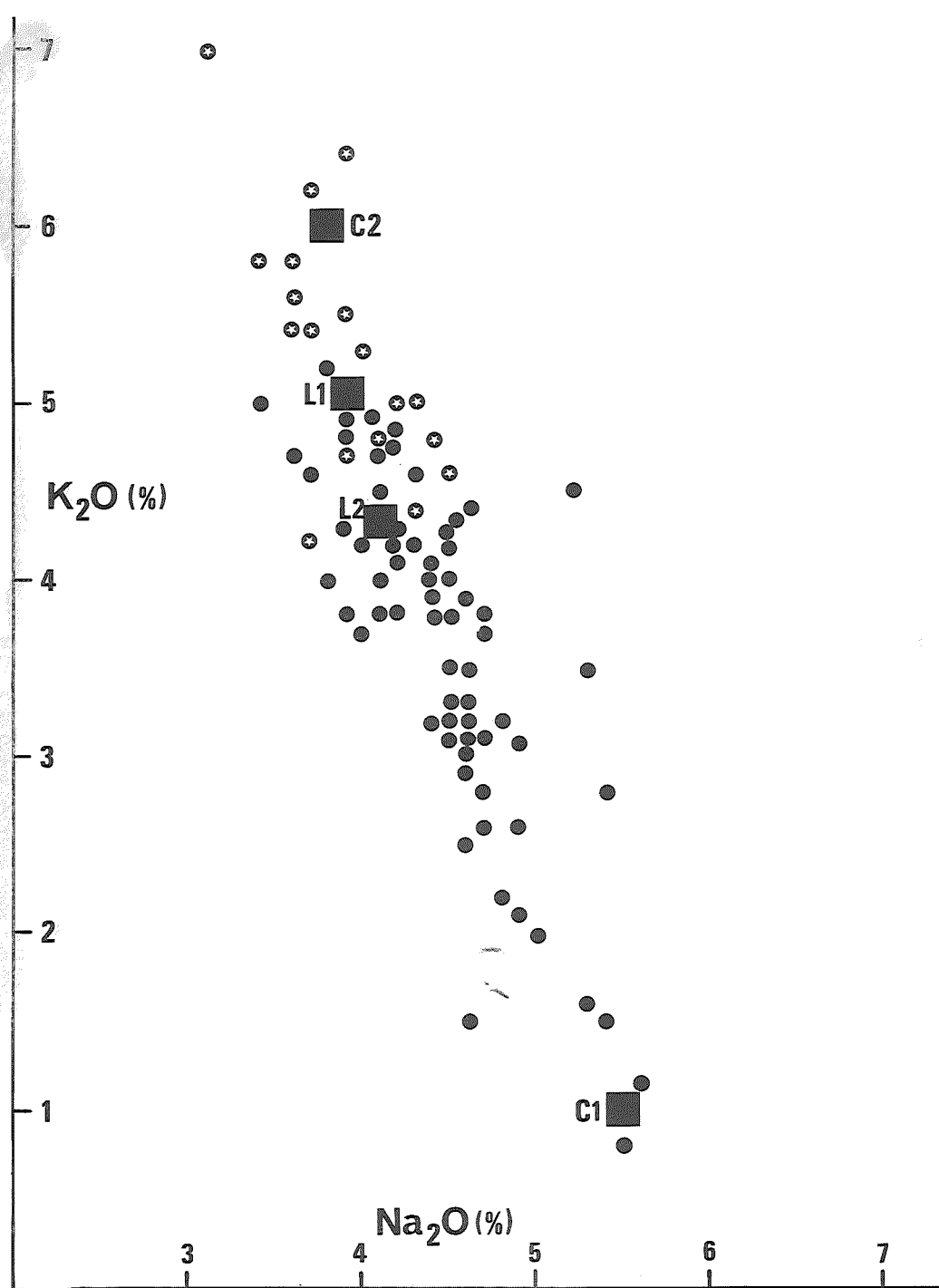

Figure 7 : The Na_2O/K_2O relationships in the two types of Nelspruit Porphyritic Granite. C1 and L1 are the calculated average cumulate and melt compositions, respectively, for the first stage of fractionation, involving plagioclase, quartz, and biotite, while C2 and L2 are the cumulate and melt compositions, respectively, for the second stage, in which plagioclase, feldspar, quartz, and biotite crystallize. The spread in the data for each type is due to the variation in the proportion of respective cumulate and melt. Symbols the same as in Figure 6.
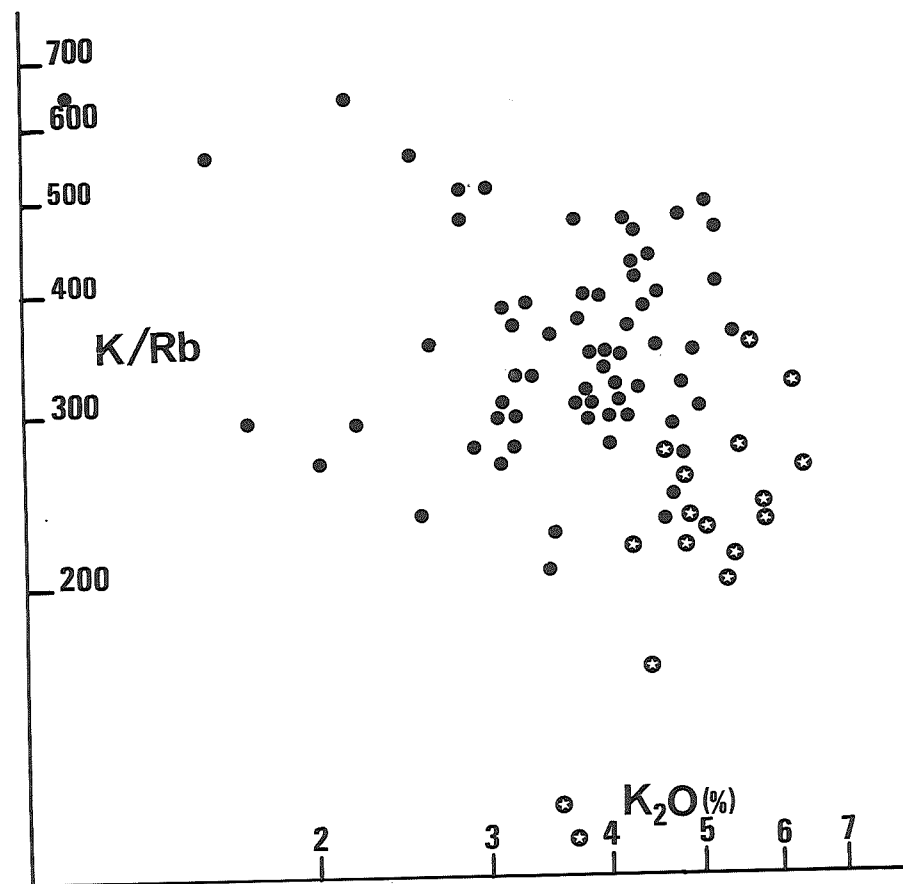
- 10 -

Figure 8 : *The relationship between K/Rb and K₂O in the two types of Nelspruit Porphyritic Granite. Symbols the same as in Figure 6.*

Figure 9 : *The relationship between K/Ba and K₂O in the two types of Nelspruit Porphyritic Granite. Symbols the same as in Figure 6.*
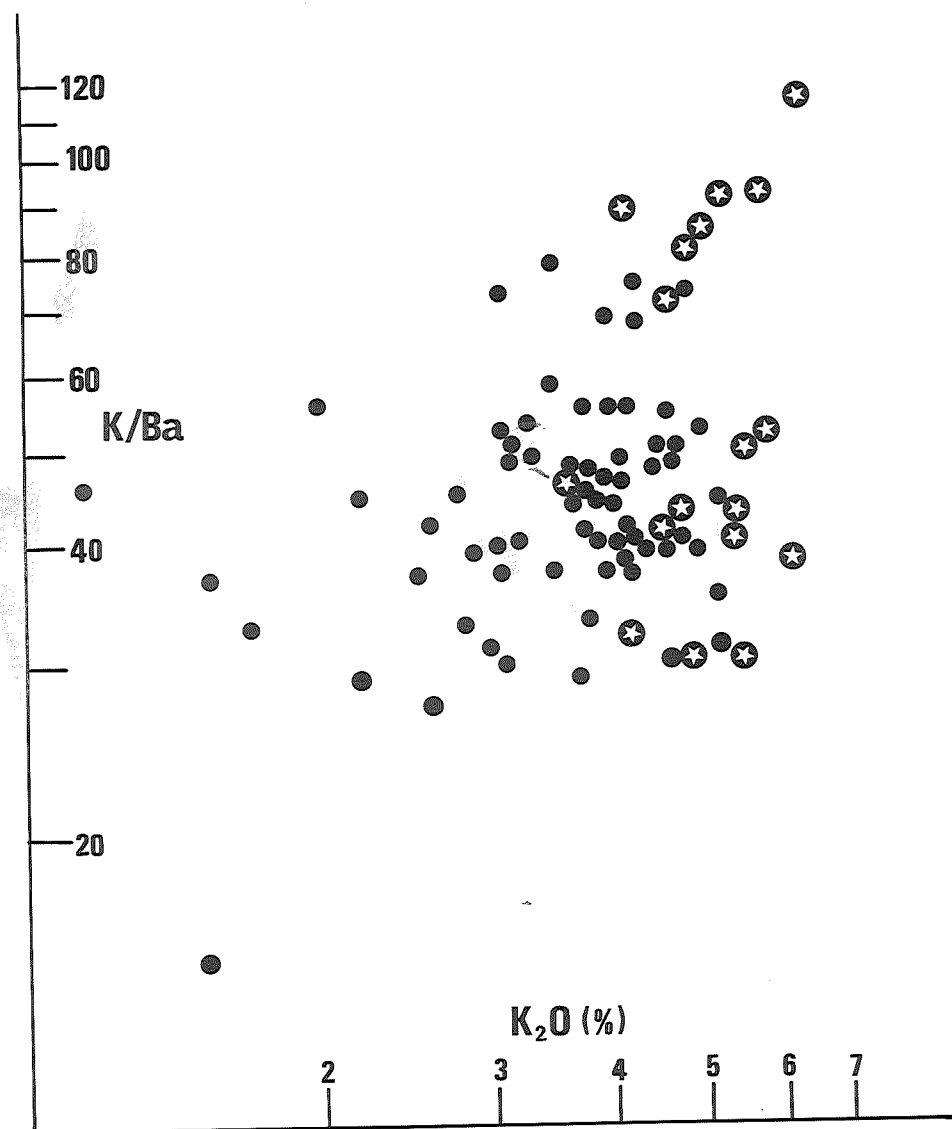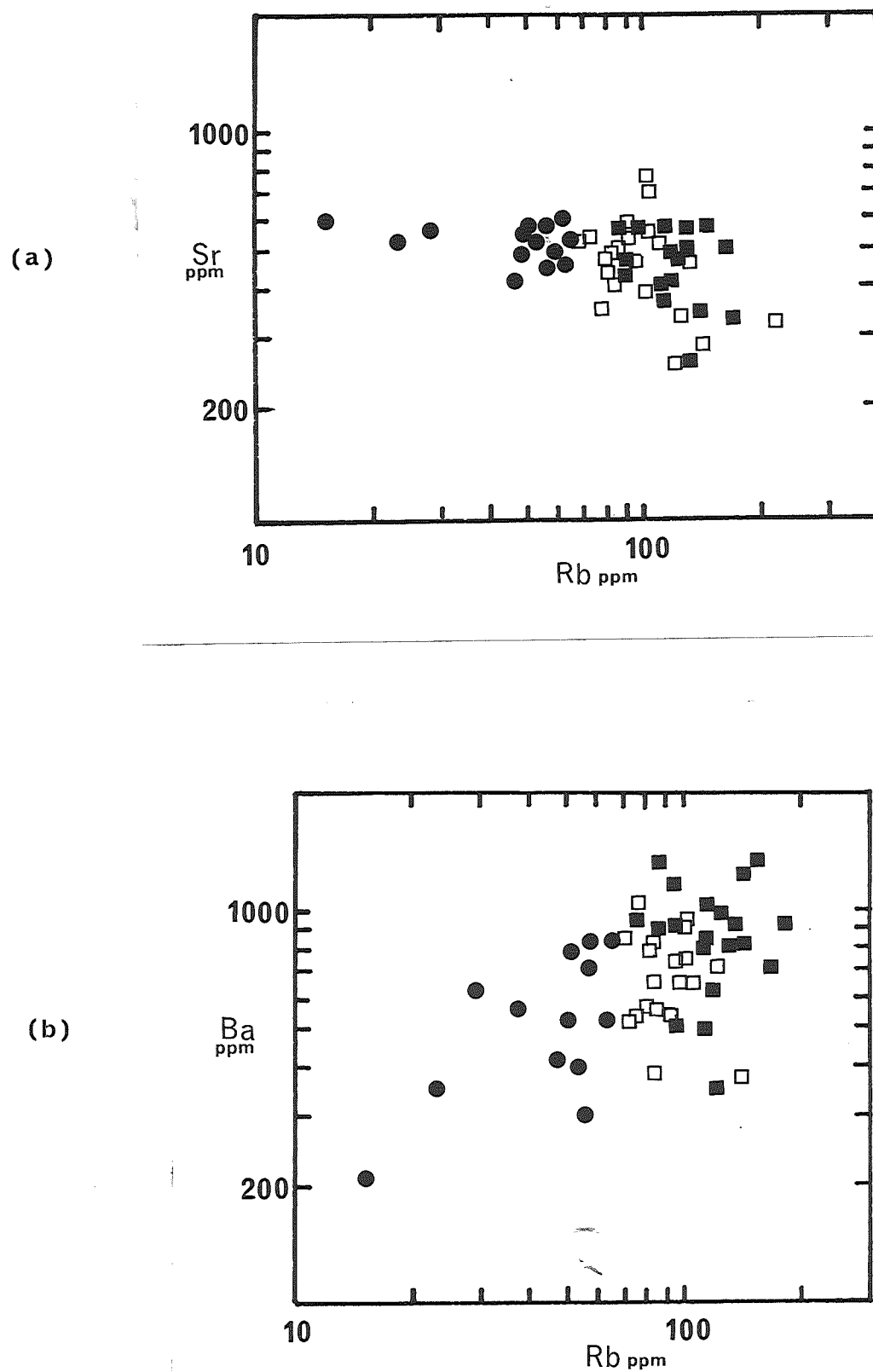
(a)

(b)

<u>Figure 10</u> : *The relationship between Sr and Rb (a), Ba and Rb (b), and K$_2$O content in the samples of Nelspruit Porphyritic Granite formed during plagioclase-quartz-biotite fractionation. Solid circles denote samples with less than 3% K$_2$O, open squares 3 to 4% K$_2$O and solid squares greater than 4% K$_2$O.*

(d) Discussion

The intimate association of the two sub-types of Nelspruit Porphyritic Granite in the field, with a total absence of distinct contact phenomena, coupled with their virtually identical appearance and the fact that both types lie on the same whole rock Rb/Sr isochron (E. Barton, personal communication), suggests that these two types are closely related.

The similarity between the trace element inter-relationships shown in Figures 6 and those modelled in Figure 1 suggests that the Nelspruit Porphyritic Granite represents a cumulate, the latter reflecting a change from entirely intercumulus K-feldspar to cumulus plus intercumulus K-feldspar. Thus, the earliest record of crystallization indicates a liquid on the plagioclase-quartz surface, crystallizing these minerals (plus biotite), and resulting in increasing Ba and

Rb and decreasing Sr abundance with fractionation (compare Figure 6 with trends AB and DE in Figure 1).

It is clear that the scatter in the data points on the plagioclase-quartz-biotite branch of the Ba vs Rb plot (solid circles of Figure 6) is greater than predicted simply by variations in the proportions of cumulus to intercumulus components. By contrast, the plot of Sr vs Rb (plagioclase-quartz-biotite branch) is comparatively well-defined. Part of the scatter is undoubtedly analytical in origin. Much of it may, however, be due to the non-representative nature of the samples, particularly with respect to biotite, which is an important host for both Ba and Rb. The effect of variation in cumulus biotite content in mixed cumulus-intercumulus assemblages is illustrated in Figure 1. In this figure, point H is the composition of the biotite in cumulate D. As the melt and cumulate change composition towards B and E respectively, the biotite changes composition towards I. Point K is a mixed assemblage comprised of 50% of cumulate E, and 50% of melt B. The addition of 5% additional biotite (of composition I) to K results in composition L, while addition of 10% biotite results in composition M. In the case of the Sr vs Rb plot, the presence of this additional biotite (or deficiency of cumulus biotite) causes displacement of points along the trend (i.e. parallel to AB), while in the case of the Ba vs Rb plot (Figure 1) displacement of points is oblique to the direction of the broad trend. This results in an apparently greater amount of scatter on a plot of Ba vs Rb than on one of Sr vs Rb (Figure 6).

Associated with increasing Ba and Rb and decreasing Sr is an increase in K_2O content. This is illustrated in Figure 10, where points on Sr vs Rb and Ba vs Rb diagrams have been ranked according to K_2O content. The generally high content of crystallized intercumulus melt, coupled with the fact that lines of constant K_2O content are asymptotic on the cumulate composition, has resulted in this general increase in K_2O (compared with Figure 2).

The Na_2O and K_2O contents of the cumulus assemblage responsible for the plagioclase-quartz (plus biotite) fractionation trend were estimated, on the assumption that the relative proportions of cumulus minerals was identical to that used to derive the relevant trend in Figure 1, and that the plagioclase contained 1,2% K_2O in solid solution. This composition is shown in Figure 7 (point C1). An average melt composition for this trend was calculated using an average of 60% intercumulus melt in the rocks comprising this trend (point L1, Figure 7). The inferred solid and melt composition straddles the observed compositional field of the samples (Figure 7), and variations in the proportions of these two end members result in the observed wide variation in Na_2O/K_2O ratio.

The plots of K/Rb and K/Ba vs K_2O (Figures 8 and 9 respectively) are broadly compatible with the predicted relationships (Figures 3 and 4) although samples representative of the plagioclase-quartz-biotite branch show more scatter than the predicted relationships. A simple model involving a cumulate of fixed mineralogical composition, mixed in varying proportions with intercumulus melt, should result in compositions lying in the wedge-shaped area DEBA on a plot of K/Rb vs K_2O or K/Ba vs K_2O (Figures 3 and 4 respectively). The actual data for the plagioclase-quartz-biotite fractionation branch show considerable scatter and do not define wedge-shaped patterns (Figures 8 and 9). As discussed with reference to the trace element inter-relationships, this scatter is partly analytical in origin, but may also be due to non-uniform distribution of cumulus biotite. In Figures 3 and 4, the composition of equilibrium biotites are shown, based on an assumed K_2O content of 10,5%. Point H is the biotite in equilibrium with melt A, while I is the biotite in equilibrium with melt B. K is a 50-50 mix of melt B and cumulate E. The addition of 5% of biotite I to K results in composition L, while the addition of 10% biotite to K results in composition M. Thus, variation in the amount of cumulus biotite will cause broadening of the point of the wedge. Actual samples with less than 20% intercumulus melt are likely to be rare (McCarthy and Hasty, 1976), so that samples will scatter between the 20% line and AB (Figures 3 and 4), and an additional component of scatter in the direction of M will be present due to the inhomogeneous distribution of biotite.

The second period of fractionation experienced by the Nelspruit Porphyritic Granite involved K-feldspar, plagioclase, quartz, and minor biotite as cumulus phases and resulted in trends of decreasing Sr and Ba with increasing Rb (Figure 6, compare with Figure 1).

The Na_2O and K_2O contents of the cumulus assemblage responsible for this trend as well as the average melt composition, have been calculated, and these are shown in Figure 7 (points C2 and L2 respectively). These points straddle the spread in the data for this trend and indicate that variations in proportion of mixing of two end members of such composition could account for the observed spread in the data. Significantly, the spread in the Na_2O/K_2O ratio is far smaller than K-feldspar is a cumulus phase than when it is not (Figure 7), this being a consequence of the difference in composition between melt and cumulate. It should be noted in relation to Figure 7, that although there is considerable uncertainty in the calculated melt and cumulate composition, L1 is slightly more potassic than L2, which is in accordance with the experimental data (Winkler, 1976).

The K/Rb ratios (Figure 8) of those samples belonging to the trend involving cumulus K-feldspar are, on average, lower than those involving only intercumulus K-feldspar. Furthermore, there is a suggestion of a positive correlation between K/Rb and K_2O, as predicted by the model (compare Figures 3 and 8).

IV. CONCLUSION

The cumulate character of granites is not easily discernible petrographically. However, trace element abundance relationships provide a means of recognizing this characteristic. Furthermore, such abundance patterns can be used to quantitatively estimate cumulus mineralogy, although at present the accuracy of such calculation is limited by uncertainties in the values of the partition coefficients.

The cumulate nature of granitic rocks results in some rather unusual chemical characteristics, the most important of which is the discontinuous nature of the trace element abundance patterns in situations where a major change in cumulus mineralogy has occurred. In cases when K_2O is not present in a major cumulus phase, variation in the proportion of cumulus to intercumulus material results in wide scatter in the Na_2O/K_2O ratio, and a sequence of decreasing Na_2O/K_2O ratio may have little or no genetic significance at all. Inter-element ratios such as K/Rb and K/Ba are controlled by extremely complex interactions between cumulus and intercumulus phases, which invariably result in considerable scatter in the data, and severely limit the amount of genetically useful information which can be extracted.

The model developed in this work is a relatively simple case, although it is evident that the results obtained from a natural example fit the model reasonably well. However, a certain amount of scatter occurs which is outside the predicted limits, indicating deviation from the model. This deviation may be partly ascribed to uncertainties in the partition coefficients and partly to analytical uncertainties. Furthermore there is little doubt that the inhomogeneous distribution of minor cumulus biotite has played an important part in introducing scatter.

ACKNOWLEDGEMENTS

REFERENCES

Cherry, R.D., Hobbs, J.B.M., Erlank, A.J. and Willis, J.P. (1970). Thorium, uranium, potassium, lead, strontium and rubidium in silicate rocks by gamma spectroscopy and/or X-ray fluorescence. Canad. Spectoscopy, 15: 1-8.

Condie, K.A. and Hunter, D.R. (1976). Trace element geochemistry of Archean granitic rocks from the Barberton region, South Africa. Earth Planet. Sci. Lett., 29: 389-400.

Emeleus, C.H. (1963). Structural and petrographic observations on layered granites from southern Greenland. Spec. Paper, Min. Soc. Amer., 1: 22-29.

Greenland, L.P. (1970). An equation for trace element distribution during magmatic crystallization. Amer. Min., 55: 455-465.

Hunter, D.R. (1973). The granitic rocks of the Precambrian in Swaziland. Spec. Publ. geol. Soc. S. Afr., 3: 131-145.

Hunter, D.R. (1974). Crustal development in the Kaapvaal craton - I - The Archaean. Precambrian Res., 1: 259-294.

McCarthy, T.S. (1976). Chemical interrelationships in a low pressure granulite terrain in Namaqualand, South Africa, and their bearing on granite genesis and the composition of the lower crust. Geochim. Cosmochim. Acta., 40: 1351-1358.

McCarthy, T.S. and Hasty, R.A. (1976). Trace element distribution patterns with reference to the crystallization of granitic melts. Geochim. Cosmochim. Acta., 40: 1057-1068.

Neumann, H., Mead, J. and Vitaliano, C.J. (1954). Trace element variation during fractional crystallization as calculated from the distribution law. Geochim. Cosmochim. Acta., 6: 90-99.

Robb, L.J. (1977). The geology and geochemistry of the Archaean granite-greenstone terrane between Nelspruit and Bushbuckridge, Eastern Transvaal. Unpub. M.Sc. Thesis, Univ. Witwatersrand.

Smith, T.E. (1974). The geochemistry of the granitic rocks of Halifax County, Nova Scotia. Can. J. Earth Sci., 12: 456-463.

Viljoen, M.J. and Viljoen, R.P. (1969). The geochemical evolution of the granitic rocks of the Barberton region. Spec. Publ. geol. Soc. S. Afr., 2: 189-218.

Visser, H.N. and Verwoerd, W.J. (1960). The geology of the country north of Nelspruit. Explanation of Sheet 22 (Nelspruit). Geol. Surv. S. Afr., 128 pp.

Winkler, H.G.F. (1976). Petrogenesis of Metamorphic Rocks. Springer-Verlag, New York, 4th Ed., 334 pp.

Wolhuter, L.E. (1973). Major and trace elements in the Opemisca Lake granite pluton, Quebec, Canada. Spec. Publ. geol. Soc. S. Afr., 3: 387-410.

* * * * * * * * * * * * * * * * * * * *